(e,2e) ionization-excitation of H2

($e,2e$) ionization-excitation of H$_2$

M. Takahashi,* Y. Khajuria, and Y. Udagawa

Institute of Multidisciplinary Research for Advanced Materials, Tohoku University, Sendai 980-8577, Japan
(Received 28 May 2003; published 22 October 2003)

Binary ($e,2e$) measurements are reported for ionization-excitation processes of H$_2$. The experiments were performed at impact energies of 1200, 1600, and 2000 eV using an energy- and momentum-dispersive spectrometer. Momentum profiles for transitions to the $2s\sigma_g$ and $2p\sigma_u$ excited final ion states are presented as normalized intensities relative to the cross section of the primary ionization to the $1s\sigma_g$ ground ion state. The results are compared with theoretical calculations of Lermer *et al.* [Phys. Rev. A **56**, 1393 (1997)] using the first-order plane-wave impulse approximation. Certain features of the discrepancies between experiment and theory can be explained by incorporating contributions from the second-order two-step mechanisms into the ($e,2e$) cross sections. Furthermore, the present results suggest that $2s\sigma_g$ and $2p\sigma_u$ cross sections approach their high-energy limits in different ways.

I. INTRODUCTION

The binary ($e,2e$) technique, also known as electron momentum spectroscopy (EMS), is now a well-established technique to investigate the electronic structure of a target atom or molecule [1–4]. The ion recoil momentum p and the electron binding energy E_{bind} can be determined by coincident detection of the two outgoing electrons with the aid of the laws of conservation of linear momentum and energy:

$$p = k_0 - k_a - k_b \tag{1}$$

and

$$E_{\text{bind}} = E_0 - E_a - E_b. \tag{2}$$

Here the k_j's and E_j's ($j = 0,a,b$) are momenta and kinetic energies of the incident and two outgoing electrons, respectively. Within the plane-wave impulse approximation (PWIA) [1], the EMS cross section for a gaseous target is proportional to the spherically averaged square of the overlap of the initial neutral (N electron) and final ion [($N-1$) electron] wave functions, which is usually called the momentum profile,

$$\sigma_{\text{EMS}} \propto \int |\langle p\Psi_f^{N-1}|\Psi_i^N\rangle|^2 d\Omega_p. \tag{3}$$

The momentum space target-ion overlap can be evaluated using configuration-interaction descriptions of the many-body wave functions.

The hydrogen molecule H$_2$ is one of the most thoroughly explored targets, because it is simple enough to be the subject of accurate calculations. Of special interest are simultaneous ionization-excitation processes of the molecule, as they can directly probe electron correlation in the target ground state. Since electron correlation is absent in the one-electron final ion state, any ionization-excitation processes

do not occur unless correlation is included in the target initial wave function; they occur by the shake-up mechanism within the framework of the PWIA. Despite the importance of the processes, however, most of the previous experiments have been limited to the primary ionization process that leaves the residual H$_2^+$ ion in the $1s\sigma_g$ ground state. The scarcity of studies for transitions to excited ion states [5–8] can be accounted for by the experimental difficulties, namely extremely small cross sections involved and the repulsive nature of the final ion states that cause significant overlaps in energy among them.

The first experimental EMS study on ionization-excitation of H$_2$ was carried out by Weigold *et al.* [5] at an impact energy of 1200 eV using a single-channel spectrometer. They have reported momentum profiles measured at binding energies of 31.5, 37.0, and 40.5 eV, where transitions to the $2p\sigma_u$, $2p\pi_u$, and $2s\sigma_g$ excited ion states dominantly contribute to the EMS cross sections, respectively. Calculations using the McLean configuration-interaction wave function [9] have been found to give unsatisfactory agreement with the experiment. The most recent study was performed by Lermer *et al.* [8] at an impact energy of 1200 eV using a momentum-dispersive spectrometer. They have measured momentum profiles at binding energies of 32.5 and 40.2 eV, where dominant contributions for the EMS cross sections arise from the transitions to the $2p\sigma_u$ and $2s\sigma_g$ states. Furthermore, highly accurate PWIA calculations based on a full configuration-interaction wave function of H$_2$ have been made and compared with the momentum profiles, showing remarkable discrepancies between experiment and theory. While the $2s\sigma_g$ profile is as expected from the theoretical prediction (except that the observed intensity is higher by about 35%), the $2p\sigma_u$ profile has displayed a significant difference in both intensity and shape. Similar measurements have been made for D$_2$ and the results have been found to be indistinguishable from the experiment with H$_2$, indicating that the nuclear motion has little effect on the momentum profiles. Consequently, Lermer *et al.* [8] have concluded that the discrepancies between experiment and theory may be due to a failure of the PWIA description of the processes, sug-

---

*Present address: Institute for Molecular Science, Okazaki 444-8585, Japan.

gesting a requirement of theoretical calculations incorporating higher-order two-step (TS) terms to reproduce the experiment.

Clearly, further investigations of the ionization-excitation of H_2 are called for to clarify the origin of the discrepancies between experiment and theory and to identify the range of the validity of the PWIA for the processes. Experiments at higher impact energies and at higher statistical precision would be desired to resolve these issues, though the extremely small cross sections of the processes make such studies difficult with the instrumentation employed so far. Very recently, we have developed an energy- and momentum-dispersive spectrometer [10] by the use of a spherical analyzer equipped with position-sensitive detectors. Because of its ability for simultaneous detection in energy and momentum, collection efficiency for the two outgoing electrons has been significantly improved compared with our previous apparatus [11]. In the present work, the newly developed spectrometer has been applied to the ionization-excitation of H_2. The measurements have been carried out at impact energies of 1200, 1600, and 2000 eV. Much higher statistics of the experiments are marked compared with the previous studies [5–8], allowing us to obtain individual momentum profiles for the transitions to the $2s\sigma_g$ and $2p\sigma_u$ states by deconvolution. The results are compared with the PWIA calculations of Lermer *et al.* [8] to discuss and to clarify the origin of the discrepancies between experiment and theory. They are also used to examine how the ionization-excitation processes approach the high-energy limits.

II. EXPERIMENTAL METHOD

EMS is a high-energy electron-impact ionization experiment in which the kinematics of all the electrons are fully determined. Under the symmetric noncoplanar scattering geometry, two outgoing electrons having equal energies and making equal polar angles of 45° with respect to the incident electron beam are detected in coincidence. Then the magnitude of the recoil ion momentum p can be determined by measurement of the out-of-plane azimuthal angle difference between the two outgoing electrons [1–4].

A detailed description of the spectrometer used in the present work has been given elsewhere [10]. Briefly, it consists of an electron gun, a set of electrostatic lens systems, a spherical analyzer, and a pair of position-sensitive detectors. Since a spherical analyzer maintains azimuthal angles for energy-analyzed electrons, use of position-sensitive detectors makes it possible to simultaneously measure energy and angle correlations between the two outgoing electrons. Thus three-dimensional EMS data can be collected at a fixed impact energy, which are constituted by relative cross sections (coincidence counts) measured as a function of binding energy and recoil ion momentum. This technique significantly increases the accuracy of the data compared with the conventional single-channel measurements, as drifts in electron beam current and fluctuations in target gas density affect all channels in the same way.

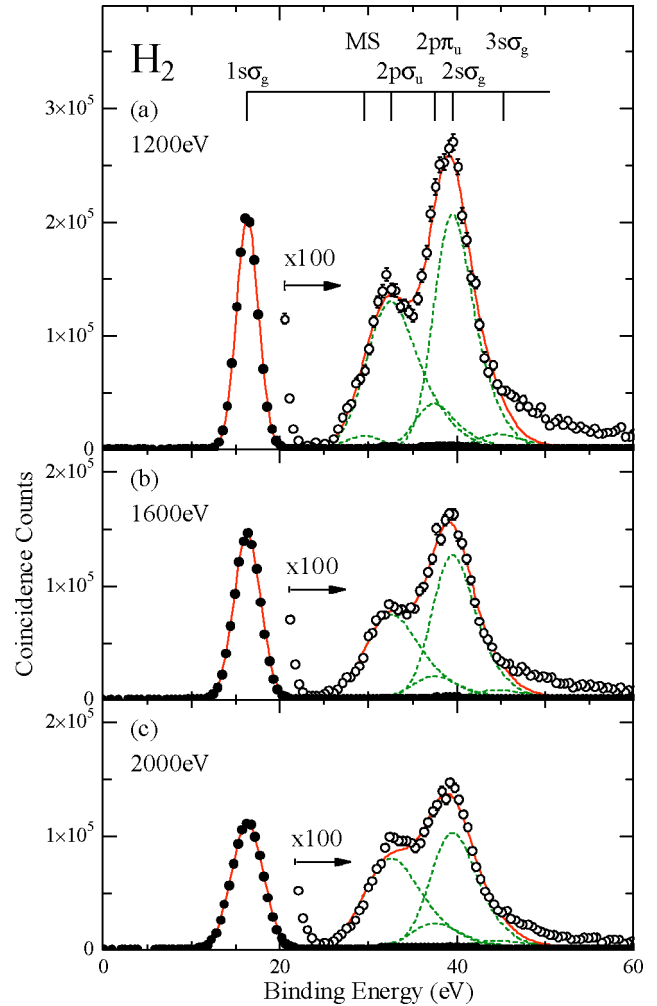In the experiments, commercially available H_2 gas (Nip-

FIG. 1. Binding-energy spectra of H_2 obtained at impact energies of (a) 1200, (b) 1600, and (c) 2000 eV. Deconvoluted curves are shown as broken lines and their sum as solid lines. MS represents contributions from multiple scattering.

pon Sanso, $>99.99999\%$) was used. The measurements were carried out at impact energies of 1200, 1600, and 2000 eV, while keeping an ambient sample gas pressure at 3.0×10^{-6} Torr. To cover a wider binding energy range at the same time, no preretardation was attempted for the outgoing electrons. The instrumental energy and momentum resolutions were then 2.6, 3.3, and 4.0 eV full width at half maximum and about 0.20, 0.23, and 0.26 a.u. at impact energies of 1200, 1600, and 2000 eV, respectively.

III. RESULTS

A. Binding-energy spectra

Binding-energy spectra of H_2 measured at impact energies of 1200, 1600, and 2000 eV are shown in Fig. 1. The spectra were obtained by summing all coincidence signals over the entire azimuthal angle difference range covered. For ease of comparison, the data responsible for ionization-excitation are scaled by a factor of 100. Franck-Condon overlaps for transitions to the excited ion states as well as the ground ion state

were calculated with the BCONT program [12] using the relevant potential-energy curves of H$_2$ and H$_2^+$ of Sharp [13]. The resultant transition profiles, folded with the instrumental energy resolutions, were subsequently employed for deconvolution. In the deconvolution procedure, contributions from multiple scattering were assumed, as in the data analysis of Lermer *et al.* [8]. Multiple scattering processes should primarily involve forward scattering by a hydrogen molecule, followed by a binary (*e*,2*e*) collision with a different hydrogen molecule. Hence their transition profiles in the binding-energy spectra were estimated using the optical oscillator strength data of H$_2$ [14]. The best fits to the present experiments are shown in the figures as broken and solid lines for the deconvoluted curves and their sum. It is evident that contributions from multiple scattering are very small, partly due to the open architecture of our spectrometer, and that the transitions to the $2s\sigma_g$ and $2p\sigma_u$ ion states exhibit relatively large cross sections compared with other ionization-excitation processes. A similar fitting procedure was employed for a series of binding-energy spectra at each azimuthal angle difference to produce momentum profiles for the transitions to the $1s\sigma_g$, $2s\sigma_g$, and $2p\sigma_u$ final ion states. Note that the profiles for the three transitions share a common intensity scale.

B. Momentum profiles and cross-section ratios

In Figs. 2, 3, and 4 we show experimental momentum profiles, obtained at impact energies of 1200, 1600, and 2000 eV for the transitions to the $1s\sigma_g$, $2s\sigma_g$, and $2p\sigma_u$ states, respectively. Also included in the figures are the PWIA calculations of Lermer *et al.* [8], which have been digitized from the literature and folded with the momentum resolutions of the spectrometer used in the present study. Since an absolute cross section cannot be determined with EMS, the $1s\sigma_g$ momentum profiles at individual impact energies were normalized to the areas of the corresponding theoretical ones. The scaling factors thus obtained were applied to the momentum profiles for ionization-excitation. Hence the $2s\sigma_g$ and $2p\sigma_u$ profiles exhibit normalized intensities relative to the $1s\sigma_g$ primary ionization cross section. The results at 1200 eV are in good accord with those of Lermer *et al.* [8], except that the $2p\sigma_u$ profile observed here shows about 60% higher intensity.

In Fig. 5, ratios of the cross section of the ionization-excitation to that of the primary ionization are plotted for the transitions to the $2s\sigma_g$ and $2p\sigma_u$ states as a function of impact energy. The ratios were obtained by summing all the intensities of the individual momentum profiles over the momentum range up to 2 a.u. and by dividing the summed intensities by that of the $1s\sigma_g$. Associated theoretical values were estimated from the PWIA calculations of Lermer *et al.* [8]. The calculated ratios are shown as broken and chain lines for the $2s\sigma_g$ and $2p\sigma_u$ channels, indicating their high-energy limits. Also included in the figure are the corresponding ratios of Edwards *et al.* [15] by electron-impact, which have been obtained by measurement of the kinetic energy release of fragment ions at 90° relative to the projectile direction. Hence their data may correspond to total (*e*,2*e*)
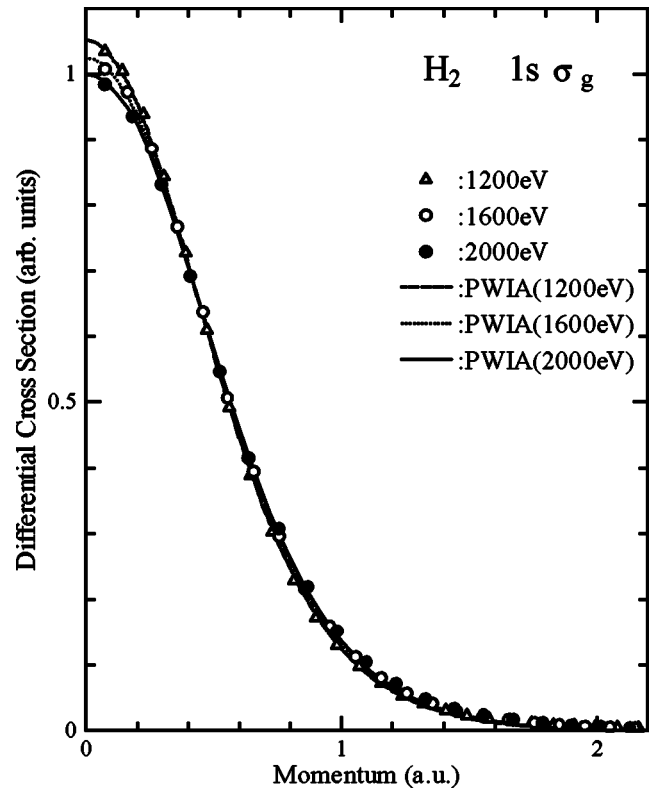

FIG. 2. Experimental momentum profiles of H$_2$ for the transition to the $1s\sigma_g$ ground ion state at impact energies of 1200, 1600, and 2000 eV. The broken, dotted, and solid lines are the PWIA calculations of Lermer *et al.* [8], which have been folded with the present momentum resolutions at 1200, 1600, and 2000 eV, respectively.

cross-section ratios integrated not only over scattering angles of the two outgoing electrons but also over all possible energy sharing between them.

IV. DISCUSSION

A. Comparison of momentum profiles between experiment and PWIA

It is immediately clear from Fig. 2 that agreement between experiment and theory is satisfactory for the transition to the $1s\sigma_g$ ground ion state at every impact energy used; the $1s\sigma_g$ momentum profile exhibits no variations with impact energy, except for slight changes due to the finite momentum resolution effects. This observation is consistent with earlier studies [7,8,16–18] that the PWIA provides a very good description of the binary (*e*,2*e*) reaction for the primary ionization process of H$_2$ at impact energies above 300 eV.

In contrast to the above result, the $2s\sigma_g$ and $2p\sigma_u$ experimental profiles in Figs. 3 and 4 are substantially different from the PWIA calculations. There are two features in the observation, namely shape and intensity difference from theory. Consider shape difference first. The PWIA rigorously requests the $2s\sigma_g$ profile to exhibit *s*-type (gerade) symmetry having its maximum at the momentum origin, and the $2p\sigma_u$ profile to do *p*-type (ungerade) symmetry with zero intensity at $p=0$. Indeed, the PWIA calculations of Lermer
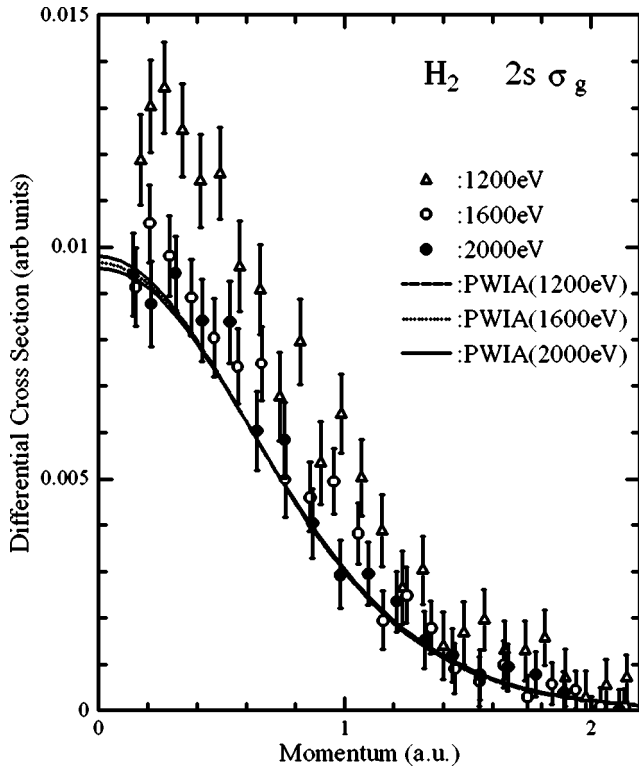
FIG. 3. Experimental momentum profiles of H_2 for the transition to the $2s\sigma_g$ excited ion state at impact energies of 1200, 1600, and 2000 eV. The broken, dotted, and solid lines are the PWIA calculations of Lermer *et al.* [8], which have been folded with the present momentum resolutions at 1200, 1600, and 2000 eV, respectively.
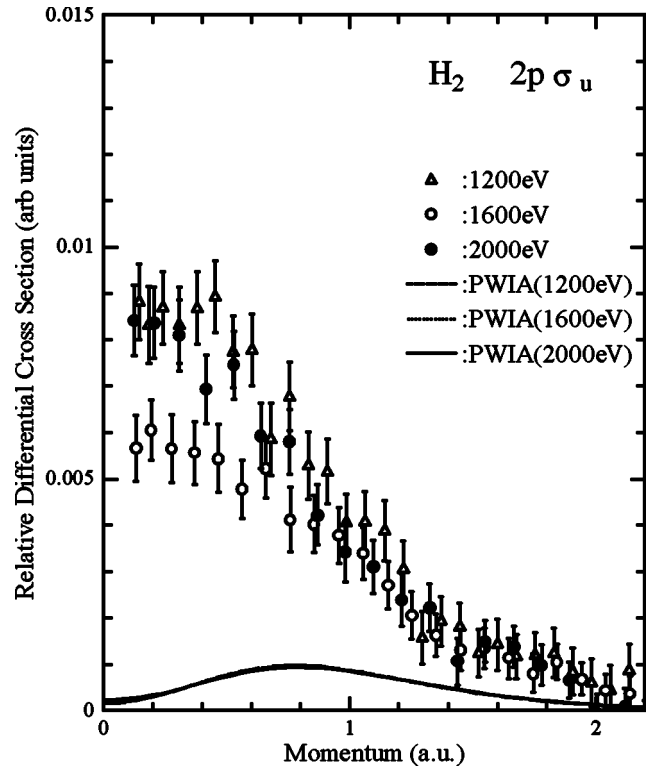
FIG. 4. Experimental momentum profiles of H_2 for the transition to the $2p\sigma_u$ excited ion state at impact energies of 1200, 1600, and 2000 eV. The broken, dotted, and solid lines are the PWIA calculations of Lermer *et al.* [8], which have been folded with the present momentum resolutions at 1200, 1600, and 2000 eV, respectively.

et al. [8] are in accordance with such symmetry consideration, with a relatively small cross section due to the finite momentum resolution effects being observed at $p=0$ for the $2p\sigma_u$ profile. On the other hand, the experiments tell us that not only the $2s\sigma_g$ but also the $2p\sigma_u$ profile always exhibits s-type symmetry. Hence it is obvious that unexpected symmetry is observed or symmetry breaking occurs for the $2p\sigma_u$ profile.

As for intensity, significant deviation of the $2p\sigma_u$ experimental profile from theory is evident, while the $2s\sigma_g$ profile also shows some discrepancies. This tendency becomes more pronounced at higher impact energy, showing remarkable variations of the cross sections with impact energy for both the $2s\sigma_g$ and $2p\sigma_u$ profiles. Surprisingly, the two profiles display a different impact energy dependence from each other. While the $2s\sigma_g$ profile shows about 50% higher intensity than the theoretical one at 1200 eV, it decreases monotonically with an increase in impact energy and closely approaches the PWIA prediction at 2000 eV. On the other hand, for the $2p\sigma_u$ profile the intensity falls off when the impact energy is raised to 1600 eV, but increases again at a higher impact energy of 2000 eV, showing "turn-up" of the cross section.

The remarkable variations of the $2s\sigma_g$ and $2p\sigma_u$ profiles with impact energy leave no doubts that noticeable contributions from higher-order terms are involved in the EMS cross sections measured. Thus the observation gives a definitive

confirmation for the conclusion of Lermer *et al.* [8] that the discrepancies between experiment and theory may be due to a failure of the PWIA description of the processes. Furthermore, since the extent of the intensity difference from the PWIA calculations would be a rough measure of contributions from higher-order terms for the EMS cross sections, the following therefore come from the present results.

(i) Symmetry breaking occurs for the $2p\sigma_u$ momentum profile.

(ii) Contributions from higher-order terms are considerably larger for the $2p\sigma_u$ profile than for the $2s\sigma_g$ one.

(iii) The $2p\sigma_u$ and $2s\sigma_g$ cross sections approach their high-energy limits in different ways.

B. Contributions from second-order terms

The plane-wave Born series model is very attractive for discussing effects of higher-order terms on the EMS cross sections, because certain contributions can be attributed to particular mechanisms of collision between projectile and target. With the help of this model, Tweed [19] has recently examined such double processes in electron-helium collision as double excitation, ionization-excitation, and double ionization, which lead to a joint change of state of both target electrons. It has been shown that the second-order Born series can be split into five terms; the first (T_2^{ai}) is related to channel coupling, the next two (T_2^{ie} and T_2^{fe}) have their
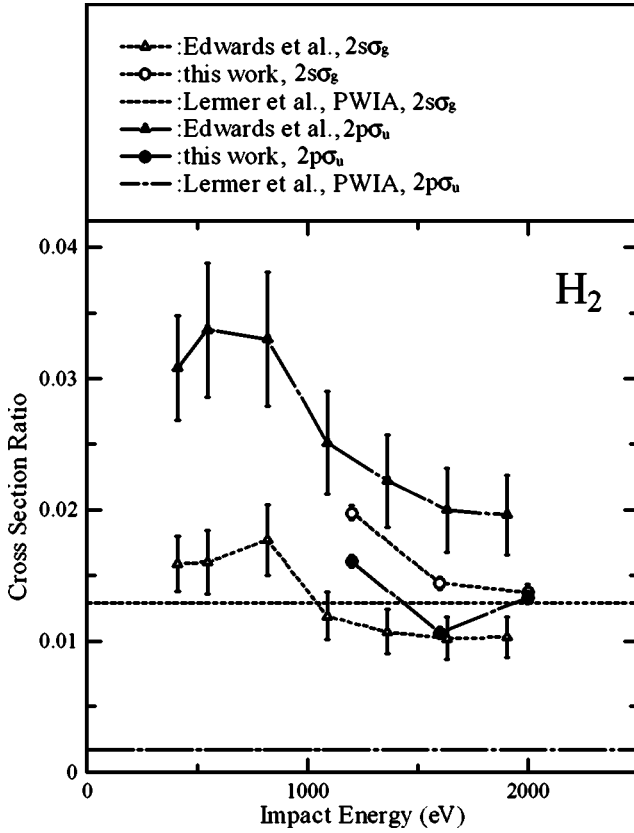
FIG. 5. Ratios of cross sections of the ionization-excitation to the primary ionization of H$_2$ for the $2s\sigma_g$ and $2p\sigma_u$ channels. Also shown are theoretical high-energy limits estimated from the PWIA calculations of Lermer *et al.* [8] and electron-impact data of Edwards *et al.* [15]. See text for details.

equivalents in first-order distorted-wave models, and the last two (T_2^{td} and T_2^{pd}) correspond to TS mechanisms. Among these five terms there must be the key ones responsible for the observations (i)–(iii) above.

We rule out first a possibility that the observations here originate in T_2^{ai} of Tweed [19], as interchannel coupling in the ionization continuum has been proven to be negligible in EMS [20]. This is in sharp contrast to high-energy photoionization in which target states with different angular momentum, which are close in energy, are mixed through interchannel coupling in the continuum [21].

The next two terms (T_2^{ie} and T_2^{fe}) of Tweed [19] describe elastic scattering of the projectile followed or preceded by a binary collision of the projectile with a single target electron. Clearly, with these terms, ionization-excitation processes can occur only by the shake-up mechanism, as in the first-order PWIA, while the resultant momentum profile may be modified because of the elastic scattering involved. In this regard, the role of the two terms for the ionization-excitation is, in the second-order interaction between projectile and target, probing momentum profiles of the $2s\sigma_g$ and $2p\sigma_u$ excited orbital components of the target initial wave function. The shapes of the $2s\sigma_g$ and $2p\sigma_u$ molecular orbitals are analogous to those of atomic s and p orbitals. Hence an insight into two terms can be gained from EMS studies of distorted-

wave effects on primary ionization processes of atomic s and p orbitals [1–4,22–24], as the terms have their equivalents in first-order distorted-wave models [19]. The studies have shown that while distorted-wave effects appear in the high momentum region, low momentum components ($p \lesssim 1$ a.u.) are little affected and are well described by the PWIA.

One may thus expect that PWIA calculations can predict symmetry properties of contributions for the $2s\sigma_g$ and $2p\sigma_u$ profiles from the terms (T_2^{ie} and T_2^{fe}) and roughly approximate relative intensity of their contributions to each other; the contributions for the $2p\sigma_u$ profile should exhibit p-type symmetry and smaller intensity. These expectations are, however, entirely inconsistent with the observations (i) and (ii). We therefore conclude that the two terms are not a principal source of the discrepancies between experiment and PWIA. This is supported, to some extent, by distorted-wave impulse approximation (DWIA) calculations of McCarthy and Mitroy [25] for ionization-excitation of isoelectronic atom He. It has been shown that the momentum profile by the DWIA for the transition to the $n=2$ state of He$^+$ is very similar to that obtainable by the PWIA in the low momentum region where the intensities observed here are mostly involved.

The last two terms (T_2^{td} and T_2^{pd}) of Tweed [19] thus remain, and indeed they can give satisfactory explanations for the observations, at least (i) and (ii). These terms correspond to the two-step 1 (TS1) and two-step 2 (TS2) mechanisms [26]. Under the present kinematics or the symmetric noncoplanar geometry, contributions from TS1 and TS2 are not distinguishable, as no information is available concerning symmetry of the cross sections with respect to the momentum transfer axis. Besides, the TS1 term may be treated in a similar way to the TS2 term with additional approximation of using plane waves for the ejected electron intermediate and final-state wave functions [19]. Thus we take the TS2 term as a representative of the TS mechanisms in the following discussion.

If we adopt a very simple H$_2$ wave function $\Psi_i^{N=2} = \psi_0(\boldsymbol{r}_1)\psi_0(\boldsymbol{r}_2)$, the TS2 term T_2^{pd} can be described as follows, according to the formalism and notation of Tweed [19]:

$$T_2^{pd} = 2^{-1} \int d\boldsymbol{k}(k_0^2 + 2E_0 - 2E_{0,\mu} - k^2 + i\varepsilon)^{-1}$$
$$\times (\pi K_a)^{-2} \langle \psi_{\mu'} | \exp(i\boldsymbol{K}_a \cdot \boldsymbol{r}_2) | \psi_0 \rangle$$
$$\times (\pi K)^{-2} \langle \psi_\mu | \exp(i\boldsymbol{K} \cdot \boldsymbol{r}_1) | \psi_0 \rangle. \tag{4}$$

Here $\boldsymbol{K} = \boldsymbol{k}_0 - \boldsymbol{k}$ and $\boldsymbol{K}_a = \boldsymbol{k} - \boldsymbol{k}_a$. The essential structure of Eq. (4) is not altered when a more sophisticated wave function is used. It should be noted that each of the matrix elements in Eq. (4) is similar to that of the first-order plane-wave Born model. Suppose that μ is a continuum state and that μ' is an excited state of the residual ion. Then we can clearly see simultaneous ionization-excitation by two sequential collisions of the projectile with different target electrons, namely the primary ionization process to the $1s\sigma_g$ ground ion state of H$_2^+$, followed by a single excitation process to an excited ion state from the $1s\sigma_g$ state. The excita-

tion process involved should be dominated by forward scattering under the present experimental conditions, where energies of both the incoming and outgoing electrons are very high compared with the energy loss. Hence the symmetry property of contributions from the TS term is essentially determined by the preceding primary ionization process and would show little dependence on the final ion state produced. Thus symmetry properties of contributions from this term for the $2s\sigma_g$ and $2p\sigma_u$ cross sections should be identical to each other and to that of the $1s\sigma_g$ momentum profile by the PWIA.

However, a difference between the contributions for the $2s\sigma_g$ and $2p\sigma_u$ cross sections must appear in intensity, since the excitation process to the $2s\sigma_g$ state from the $1s\sigma_g$ state is a nondipole transition whereas that to the $2p\sigma_u$ state is a dipole one. By considering again that the processes are dominated by forward scattering or pseudo-photon-impact, the magnitude of the contributions should be much larger for the "optically allowed" $2p\sigma_u$ transition than for the "optically forbidden" $2s\sigma_g$ transition. As a result, one may reach the following conclusion. The $2s\sigma_g$ profile in Fig. 3 is composed of relatively large contributions from the first-order PWIA term with s-type symmetry and small contributions from the second-order TS term with the same symmetry. Hence the symmetry of the profile is maintained, while the intensity is affected by inclusion of the TS term. On the other hand, for the $2p\sigma_u$ profile in Fig. 4, contributions from the TS term with s-type symmetry become dominant, because those from the PWIA term are significantly smaller. Thus symmetry breaking arises for the $2p\sigma_u$ profile, and the intensity is remarkably increased compared with the PWIA cross section. Unquestionably, inclusion of contributions from the TS mechanisms in the EMS cross sections can account for the observations (i) and (ii), verifying the proposition of Lermer et al. [8] that theoretical calculations incorporating the TS terms would be required to reproduce the experiment. The observation (iii) will be discussed below.

C. Impact energy dependence of cross section ratio

When the modulus squared of the sum of the first-order and second-order terms is taken to get a cross section, interference between them can occur and the cross section depends on not only their amplitudes but also their relative phases. An outstanding example of this has been reported by Edwards et al. [15] for ionization-excitation of H_2. As can be seen in Fig. 5, their ratios for the $2s\sigma_g$ and $2p\sigma_u$ channels are enhanced at around an impact energy of 750 eV. Such enhancement has been interpreted as visible proof of constructive interference between the shake-up and TS terms in a collision of a negatively charged projectile and an electron [15,27–30].

Also evident from Fig. 5 is that the ratios for the $2s\sigma_g$ and $2p\sigma_u$ channels observed here are considerably different from those of Edwards et al. [15]. In their experiment, both ratios decrease monotonically with an increase in impact energy above ~750 eV, and the $2p\sigma_u$ asymptotic value (~0.02) is larger than the $2s\sigma_g$ one (~0.01). On the other hand, in the present study, although the ratio for $2s\sigma_g$ shows

similar asymptotic behavior to the data of Edwards et al., that for $2p\sigma_u$ exhibits the "turn-up" at the highest impact energy employed, as already noted. Furthermore, the ratio for $2p\sigma_u$ is always smaller than that for $2s\sigma_g$. Besides, their high-energy limits or theoretical values estimated from the PWIA calculations of Lermer et al. [8] are different from those of Edwards et al.

Interestingly, the trend reported by Edwards et al. that the asymptotic value for $2p\sigma_u$ is larger than that for $2s\sigma_g$ coincides with the result of dissociative photoionization experiments of H_2 using several tens eV photons [31], in which the $\Sigma\rightarrow\Pi$ transitions have been found to be dominant. This coincidence is not accidental, since the total cross section by electron impact at high energy is dominated by large impact parameter (pseudo-photon-impact) collisions that eject soft electrons with continuum energies of the order of their original binding energies [27,32]. On the other hand, in the present study the experiments were performed at the Bethe ridge [33], where the so-called electron Compton scattering [34] occurs and both scattered and ejected electrons are produced with high energy. Thus the difference in ratio between the two experiments reveals a remarkable dependence of the cross section at high energy on energy sharing between the two outgoing electrons, illuminating disparity in collision dynamics.

Relative to the difference in ratio discussed above, it is much more difficult to reach an understanding of the observed asymptotic behavior. The source of the "turn-up" of the ratio for the $2p\sigma_u$ channel is unclear. To the best of our knowledge, this kind of "turn-up" has never been observed in previous studies with photons and various charged particles, including double ionization. Its peculiarity can be illustrated by referring to a theoretical model for He proposed by Popov et al. [35]. They have predicted that the ratio of maximum TS1 and shake-up contributions under the Bethe ridge conditions should be on the order of the inverse of the momentum of the outgoing electrons. Although the model appears applicable to the asymptotic behavior of the ratio for $2s\sigma_g$, it is unlikely to give any indications of the "turn-up" for $2p\sigma_u$. To resolve this issue, theoretical calculations incorporating the TS terms are needed for H_2. If the observed "turn-up" is real, it would suggest that the ratio for $2p\sigma_u$ approaches its high-energy limit, oscillating with an increase in impact energy. To confirm the observation, experiments at lower and higher impact energies are now in progress.

V. CONCLUSIONS

The present study reported a binary $(e,2e)$ study of ionization-excitation of H_2 for the transitions to the $2s\sigma_g$ and $2p\sigma_u$ excited final ion states. The experimental cross sections exhibit variations with impact energy, confirming a failure of the PWIA description of the processes. Furthermore, it has been discussed and verified that inclusion of the second-order TS mechanisms is crucial for understanding the discrepancies between experiment and PWIA. In particular, a dominant contribution from the TS mechanisms for the $2p\sigma_u$ cross section manifests itself in the momentum profile, bringing symmetry breaking. Moreover, the ratios for the $2s\sigma_g$

and $2p\sigma_u$ channels have been found to approach their high-energy limits in different ways. While the ratio for $2s\sigma_g$ decreases monotonically with an increase in impact energy, that for $2p\sigma_u$ appears to oscillate. These findings may suggest that amplitudes and relative phases of the Born terms involved largely depend not only on impact energy but also the final ion state, for which detailed theoretical explanations are needed.

[1] I. E. McCarthy and E. Weigold, Phys. Rep., Phys. Lett. **27C**, 275 (1976).

[2] C. E. Brion, Int. J. Quantum Chem. **29**, 1397 (1986).

[3] M. A. Coplan, J. H. Moore, and J. P. Doering, Rev. Mod. Phys. **66**, 985 (1994).

[4] E. Weigold and I. E. McCarthy, *Electron Momentum Spectroscopy* (Kluwer Academic/Plenum, New York, 1999).

[5] E. Weigold, I. E. McCarthy, A. J. Dixson, and S. Dey, Chem. Phys. Lett. **47**, 209 (1977).

[6] S. M. Bharathi, S. Braidwood, A. M. Grisogono, N. Persiantseva, and E. Weigold, in *International Conference on the Physics of Electron-Atom Collisions XVII, Brisbane, Australia, 1991, Abstracts of Contributed Papers*, edited by I. E. McCarthy *et al.* (Adam Hilger, Bristol, 1991).

[7] N. Lermer, B. R. Todd, N. M. Cann, C. E. Brion, Y. Zheng, S. Chakravorty, and E. R. Davidson, Can. J. Phys. **74**, 748 (1996).

[8] N. Lermer, B. R. Todd, N. M. Cann, Y. Zheng, C. E. Brion, Z. Yang, and E. R. Davidson, Phys. Rev. A **56**, 1393 (1997).

[9] A. D. McLean, A. Weiss, and M. Yoshimine, Rev. Mod. Phys. **32**, 211 (1960).

[10] M. Takahashi, T. Saito, M. Matsuo, and Y. Udagawa, Rev. Sci. Instrum. **73**, 2242 (2002).

[11] M. Takahashi, H. Nagasaka, and Y. Udagawa, J. Phys. Chem. A **101**, 528 (1997).

[12] R. J. Le Roy, Comput. Phys. Commun. **52**, 383 (1989).

[13] T. E. Sharp, At. Data **2**, 119 (1971).

[14] W. F. Chan, G. Cooper, and C. E. Brion, Chem. Phys. **168**, 375 (1992).

[15] A. K. Edwards, R. M. Wood, A. S. Beard, and R. L. Ezell, Phys. Rev. A **42**, 1367 (1990).

[16] S. Dey, I. E. McCarthy, P. J. O. Teubner, and E. Weigold, Phys. Rev. Lett. **34**, 782 (1975).

[17] J. N. Migdall, M. A. Coplan, D. S. Hench, J. H. Moore, J. A. Tossell, V. H. Smith, Jr., and J. W. Liu, Chem. Phys. **57**, 141 (1981).

[18] K. T. Leung and C. E. Brion, Chem. Phys. **82**, 113 (1983).

[19] R. J. Tweed, Z. Phys. D: At., Mol. Clusters **23**, 309 (1992).

[20] A. S. Kheifets, M. Vos, E. Weigold, M. Brunger, and I. E. McCarthy, Phys. Rev. A **58**, 2815 (1998).

[21] E. W. B. Dias, H. S. Chakraborty, P. C. Deshmukh, S. T. Manson, O. Hemmers, P. Glans, D. L. Hansen, H. Wang, S. B. Whitfield, D. W. Lindle, R. Wehlitz, J. C. Levin, I. A. Sellin, and R. C. C. Perera, Phys. Rev. Lett. **78**, 4553 (1997).

[22] A. J. Dixon, I. E. McCarthy, C. J. Noble, and E. Weigold, Phys. Rev. A **17**, 597 (1978).

[23] J. P. D. Cook, J. Mitroy, and E. Weigold, Phys. Rev. Lett. **52**, 1116 (1984).

[24] S. W. Braidwood, M. J. Brunger, D. A. Konovalov, and E. Weigold, J. Phys. B **26**, 1655 (1993).

[25] I. E. McCarthy and J. Mitroy, Phys. Rev. A **34**, 4426 (1986).

[26] T. A. Carlson and M. O. Krause, Phys. Rev. **140**, 1057 (1965).

[27] J. H. McGuire, N. Berrah, R. J. Bartlett, J. A. R. Samson, J. A. Tanis, C. L. Cocke, and A. S. Schlachter, J. Phys. B **28**, 913 (1995).

[28] J. H. McGuire, Phys. Rev. Lett. **49**, 1153 (1982).

[29] J. H. McGuire, Phys. Rev. A **36**, 1114 (1987).

[30] J. F. Reading and A. L. Ford, J. Phys. B **20**, 3747 (1987).

[31] K. Ito, R. I. Hall, and M. Ukai, J. Chem. Phys. **104**, 8449 (1996).

[32] J. H. McGuire, J. Phys. B **17**, L779 (1984).

[33] M. Inokuti, Rev. Mod. Phys. **43**, 297 (1971).

[34] R. A. Bonham and H. F. Wellenstein, in *Compton Scattering*, edited by B. Williams (McGraw-Hill, New York, 1977).

[35] Y. V. Popov, C. D. Cappello, B. Joulakian, and N. M. Kuzmina, J. Phys. B **27**, 1599 (1994).